Issue 62; December 2021

The ISHC Bulletin

Recent Publications of ISHC Members

Issue 62; December 2021

3,9-Disubstituted Bis[1]benzothieno[3,2-*b*;2′,3′-*e*][1,4]thiazines with Low Oxidation Potentials and Enhanced Emission

Henning R. V. Berens, Kausar Mohammad, Guido J. Reiss, and Thomas J. J. Müller* (thomasjj.mueller@hhu.de)

J. Org. Chem. **2021**, *86*, 8000–8014. **DOI:** 10.1021/acs.joc.1c00397

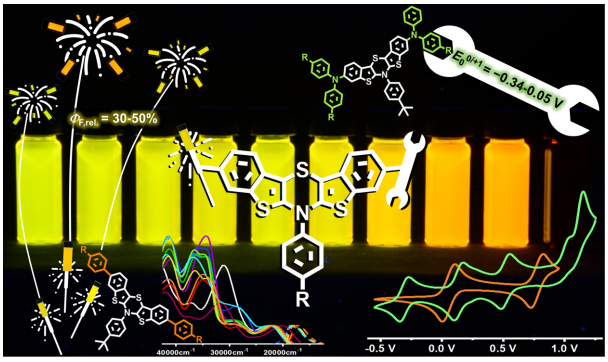

Abstract: Dibrominated bis[1]benzothieno[3,2-*b*;2′,3′-*e*][1,4]-thiazines (BBTT) are efficiently synthesized and applied in Suzuki and Buchwald–Hartwig cross-coupling reactions to give access to 3,9-disubstituted BBTT derivatives with extended π-conjugation and enhanced electronic properties. For instance, 3,9-di(hetero)aryl substituted BBTT derivatives surpass their parent congeners phenothiazines with lower oxidation potentials and pronounced yellow to orange-red fluorescence ($\Phi_f \approx 30–45\%$). In addition, 3,9-bis(di(hetero)-arylamino) substituted BBTT possess very high lying HOMO energy (E_{HOMO} = −4.46 to −4.83 eV), a favorable property of hole transport molecules. A representative X-ray structure analysis reveals that the central BBTT core in these extended π-systems is essentially planarized. Upon protonation of a 3,9-bis(di(hetero)-arylamino) substituted BBTT, the absorption color shifts from yellow to deep blue with a concomitant loss of the emission. The optical properties of these novel BBTT derivatives can be plausibly rationalized by time-dependent density functional theory (TD(DFT)) calculations and correlation between experimentally determined oxidation potentials and σ_p parameters as well as between photophysical data and the specific substituent parameter σ_p^- by establishing electronic structure–property relationships.

Direct Approach to 3-Fluoroindoles and 3,3-Difluoroindolines from 2,2-Difluoro-2-phenylethan-1-amines via C–H/N–H Coupling

Lanfei Zhang, Xiaofei Zhang, Yongmei Cui,* and Chunhao Yang* (ymcui@shu.edu.cn or chyang@simm.ac.cn)

Synthesis **2021**, *53*, 3815–3826. **DOI:** 10.1055/a-1509-8624

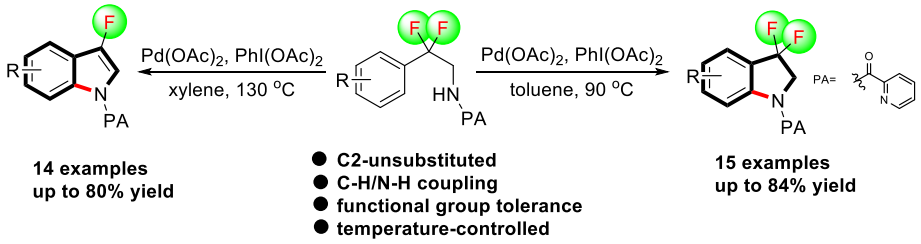

Abstract: Herein, a direct method for the synthesis of 3-fluoroindoles and 3,3-difluoroindolines from easily accessible 2,2-difluoro-2-phenylethan-1-amines was presented. This protocol was performed by Pd-catalyzed direct C–H/N–H coupling and employed picolinamide as a directing group. By controlling the temperature for this transformation, various 3,3-difluoroindolines and 3-fluoroindoles could be obtained with moderate to good yields.

Chemo- and Regioselective Cross-Dehydrogenative Coupling Reaction of 3-Hydroxycarbazoles with Arenols Catalyzed by a Mesoporous Silica-Supported Oxovanadium

Kengo Kasama, Kyohei Kanomata, Yuya Hinami, Karin Mizuno, Yuta Uetake, Toru Amaya, Makoto Sako, Shinobu Takizawa, Hiroaki Sasai, and Shuji Akai* (akai@phs.osaka-u.ac.jp)
RSC Adv. **2021**, *11*, 35342–35350. **DOI:** 10.1039/d1ra07723f

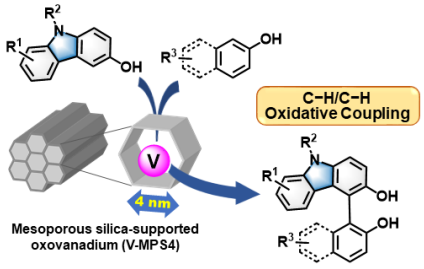

Abstract: Cross-dehydrogenative coupling between 3-hydroxycarbazoles and 2-naphthols has been achieved using a mesoporous silica-supported oxovanadium catalyst.

Studies on the Application of the Paternò–Büchi Reaction to the Synthesis of Novel Fluorinated Scaffolds

Mario Andrés Gomez Fernandez, Corentin Lefebvre, Alexander Sudau, Pierre Genix, Jean-Pierre Vors, Manabu Abe, and Norbert Hoffmann* (norbert.hoffmann@univ-reims.fr)
Chem. Eur. J. **2021**, *27*, 15722–15729. **DOI:** 10.1002/chem.202102621

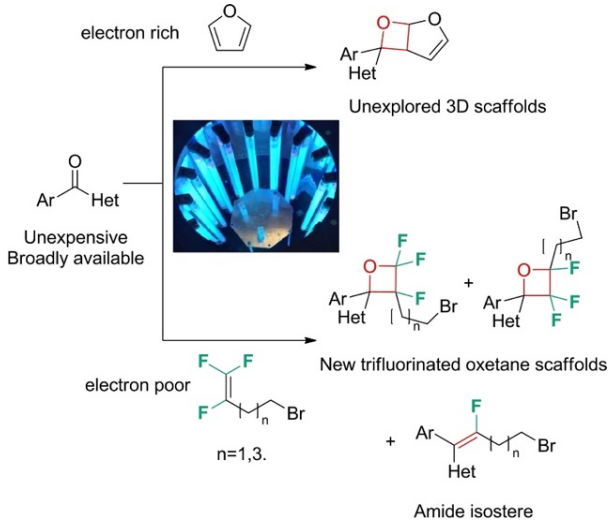

Abstract: In the context of new scaffolds obtained by photochemical reactions, Paternò–Büchi reactions between heteroaromatic, trifluoromethylphenyl ketone and electron-rich alkenes to give oxetanes are described. A comprehensive study has then been carried out on the reaction of aromatic ketones with fluorinated alkenes. Depending on the substitution pattern at the oxetane ring, a metathesis reaction is described as a minor side process to give mono fluorinated alkenes. Overall, this last reaction corresponds to a photo-Wittig reaction and yield amid isosteres. In order to explain the uncommon regioselectivity of the Paternò–Büchi reaction with these alkenes, electrostatic-potential derived charges (ESP) have been determined. In a second computational study, the relative stabilities of the typical 1,4-diradical intermediates of the Paternò–Büchi reaction have been determined. The results well explain the regioselectivity. Further transformations of the oxetanes or previous functionalization of the fluoroalkenes open perspectives for oxetanes as core structures for biologically active compounds.

Unexpected Formation of 2,2-Dichloro-*N*-(chloromethyl)acetamides During Attempted Staudinger 2,2-Dichloro-β-lactam Synthesis

Sari Deketelaere, Elias Van Den Broeck, Lore Cools, Daan Deturck, Hannes Naeyaert, Kristof Van Hecke, Christian V. Stevens, Veronique Van Speybroeck,* and Matthias D'hooghe* (veronique.vanspeybroecke@ugent.be or matthias.dhooghe@ugent.be)

Eur. J. Org. Chem. **2021**, 5823–5830. **DOI:** 10.1002/ejoc.202100975

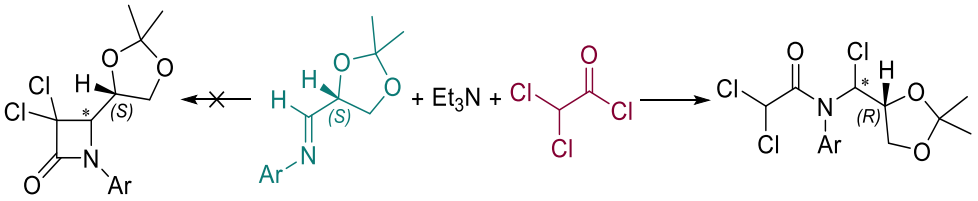

Abstract: In the quest for 3,3-dichloro-β-lactam building blocks, the serendipitous formation of 2,2-dichloro-*N*-(chloromethyl)acetamides was observed. This peculiar reactivity was investigated in detail, both experimentally and computationally by means of Density Functional Theory (DFT) calculations. 2,2-Dichloro-*N*- (chloromethyl)acetamides were thus shown to be formed experimentally through reaction of 2,2-dichloroacetyl chloride with glyceraldehyde-derived imines, i.e. (2,2-dimethyl-1,3-dioxolan-4-yl)methanimines, bearing aromatic *N*-substituents, in the presence as well as in the absence of a base. Deployment of aliphatic imines, however, resulted in complex reaction mixtures, pointing to the importance of a stabilizing aromatic substituent at nitrogen. The DFT results indicate that the substituents can alter the governing equilibria on the one hand and intrinsic barrier heights for the different routes on the other hand, showing that these are controlling the reaction outcome. Furthermore, the 2,2-dichloro-*N*-(chloromethyl)acetamides proved to be rather unstable in solution and thus difficult to isolate. Nonetheless, their molecular structure was confirmed by means of NMR analysis of several purified analogs and X-ray study of a 4-methoxyphenyl derivative.

Recent Contributions of Quinolines to Antimalarial and Anticancer Drug Discovery Research

Tim Van de Walle, Lore Cools, Sven Mangelinckx, Matthias D'hooghe* (matthias.dhooghe@ugent.be)

Eur. J. Med. Chem. **2021**, *226*, 113865 (1–70). **DOI:** 10.1016/j.ejmech.2021.113865

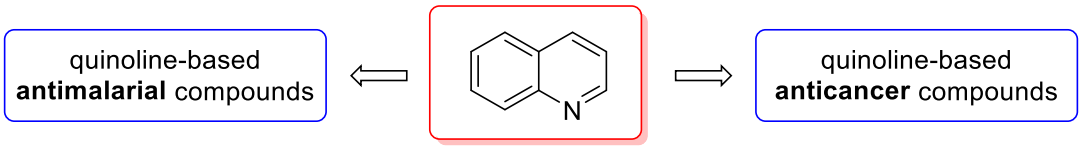

a literature overview covering papers
from the period 2018-2020

Abstract: Quinoline, a privileged scaffold in medicinal chemistry, has always been associated with a multitude of biological activities. Especially in antimalarial and anticancer research, quinoline played (and still plays) a central role, giving rise to the development of an array of quinoline-containing pharmaceuticals in these therapeutic areas. However, both diseases still affect millions of people every year, pointing to the necessity of new therapies. Quinolines have a long-standing history as antimalarial agents, but established quinoline-containing antimalarial drugs are now facing widespread resistance of the *Plasmodium* parasite. Nevertheless, as evidenced by a massive number of recent literature contributions, they are still of great value for future developments in this field. On the other hand, the number of currently approved anticancer drugs containing a quinoline scaffold are limited, but a strong increase and interest in quinoline compounds as potential anticancer agents can be seen in the last few years. In this review, a literature overview of the most recent contributions made by quinoline-containing compounds as potent antimalarial or anticancer agents is provided, covering publications between 2018 and 2020.

Tandem Oxidation-Dehydrogenation of (Hetero)Arylated Primary Alcohols via Perruthenate Catalysis

Christian J. Bettencourt, Sharon Chow, Peter W. Moore, Christopher D. G. Read, Yanxiao Jiao, Jan Peter Bakker, Sheng Zhao, Paul V. Bernhardt, and Craig M. Williams* (c.williams3@uq.edu.au)

Aust. J. Chem. **2021**, *74*, 652–659. **DOI:** 10.1071/CH21137

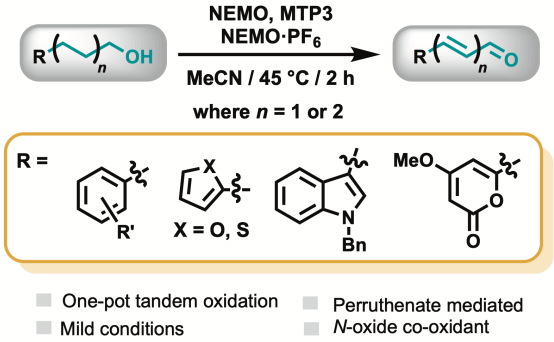

Abstract: A novel method for the scarcely reported dehydrogenation reaction of primary alcohols to give enals is presented. Modified Ley–Griffith oxidation conditions utilizing novel *N*-oxide co-oxidants, NEMO (*N*-ethylmorpholine *N*-oxide) or NEMO·PF_6 (*N*-ethyl-*N*-hydroxymorpholinium hexafluorophosphate), alongside the bench-stable perruthenate MTP3 (methyltriphenylphosphonium perruthenate), enable alcohol oxidation and subsequent dehydrogenation of the intermediate saturated aldehyde under mild conditions. A range of (hetero)arylated primary alcohols are suitable for this method providing the corresponding α,β-unsaturated or α,β,γ,δ-unsaturated aldehydes in low to moderate yields. The discovery, development, scope, and challenges of this novel method are presented together with conceivable application to polyenyl natural product total synthesis.

An Asymmetric Oxidative Cyclization/Mannich-type Addition Cascade Reaction for Direct Access to Chiral Pyrrolidin-3-ones

Su Zhou, Xiongda Xie, Xinxin Xu, Shanliang Dong, Wenhao Hu, and Xinfang Xu* (xuxinfang@mail.sysu.edu.cn)

Chem. Commun. **2021**, *57*, 12171–12174. **DOI:** 10.1039/d1cc04830a

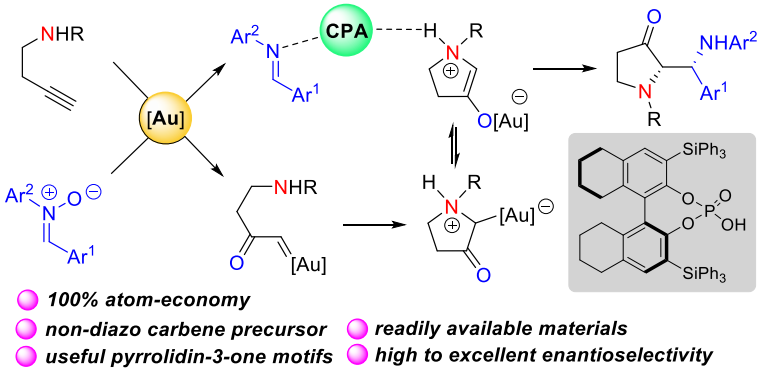

Abstract: An efficient gold and chiral phosphoric acid cooperative catalyzed enantioselective oxidative cyclization/Mannich-type addition reaction of homopropargyl amides with nitrones has been developed, which provides chiral pyrrolidin-3-ones in high yields with excellent enantioselectivities under mild conditions. This reaction employed stable and readily available alkynes as non-diazo carbene precursor, which provides a 100% atom economy method with high bond formation efficiency.

The X-ray Structures of (*R*)-2,2′-Dimethyl-1,1′-binaphthyl and (±)-2-Bromomethyl-2′-dibromomethyl-1,1′-binaphthyl

R. Alan Aitken,* Ryan A. Inwood, and Alexandra M. Z. Slawin (raa@st-and-ac.uk)

J. Chem. Crystallogr. **2021**, *51*, 497–504. **DOI:** 10.1007/s10870-020-00876-9

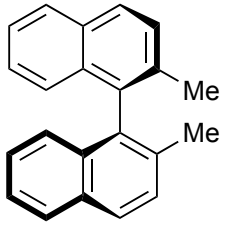

two molecules, ring torsion angle 81.9, 89.6°

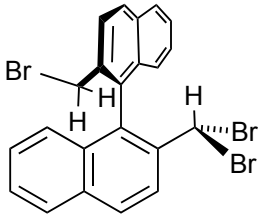

ring torsion angle 87.7°

Abstract: Molecular structures of (*R*)-2,2′-dimethyl-1,1′-binaphthyl [monoclinic, *a* = 11.24420 (11), *b* = 10.56190 (9), *c* = 13.27180 (13) Å, β = 90.7041 (9)°, space group $P2_1$] and (±)-2-bromomethyl-2′-dibromomethyl-1,1′-binaphthyl [triclinic, *a* = 9.4637 (14), *b* = 9.9721 (18), *c* = 9.9922 (19) Å, α = 100.093 (5), β = 97.141 (5), γ = 92.585 (4)°, space group *P*-1] are reported and compared with those of other simple 2,2′-disubstituted-1,1′-binaphthyls.

Enantioselective Total Synthesis of (+)-Heilonine

Kyle J. Cassaidy and Viresh H. Rawal* (vrawal@uchicago.edu)

J. Am. Chem. Soc. **2021**, *143*, 16394–16400. **DOI:** 10.1021/jacs.1c08756

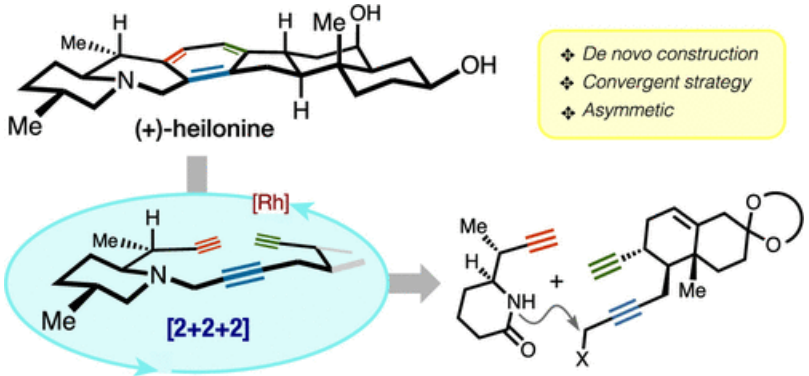

Abstract: Chemical transformations that rapidly and efficiently construct a high level of molecular complexity in a single step are perhaps the most valuable in total synthesis. Among such transformations is the transition metal catalyzed [2 + 2 + 2] cycloisomerization reaction, which forges three new C–C bonds and one or more rings in a single synthetic operation. We report here a strategy that leverages this transformation to open *de novo* access to the *Veratrum* family of alkaloids. The highly convergent approach described herein includes (i) the enantioselective synthesis of a diyne fragment containing the steroidal A/B rings, (ii) the asymmetric synthesis of a propargyl-substituted piperidinone (F ring) unit, (iii) the high-yielding union of the above fragments, and (iv) the intramolecular [2 + 2 + 2] cycloisomerization reaction of the resulting carbon framework to construct in a single step the remaining three rings (C/D/E) of the hexacyclic cevanine skeleton. Efficient late-stage maneuvers culminated in the first total synthesis of heilonine, achieved in 21 steps starting from ethyl vinyl ketone.

International Society of Heterocyclic Chemistry
ISHC

Issue 62; December 2021

Compounds from Plantar Foot Sweat, Nesting Material, and Urine Show Strain Patterns Assocaited with Agonistic and Affiliative Behaviors in Group Housed Male Mice, *Mus musculus*

Amanda J. Barabas,* Helena A. Soini, Milos V. Novotny, David R. Williams, Jacob A Desmond, Jeffrey R. Lucas, Marisa A. Erasmus, Heng-Wei Chang, Brianna N. Gaskill (abarabas@purdue.edu)
PLoS ONE **2021**, *16*, e0251416 (1–29). **DOI:** 10.1371/journal.pone.0251416

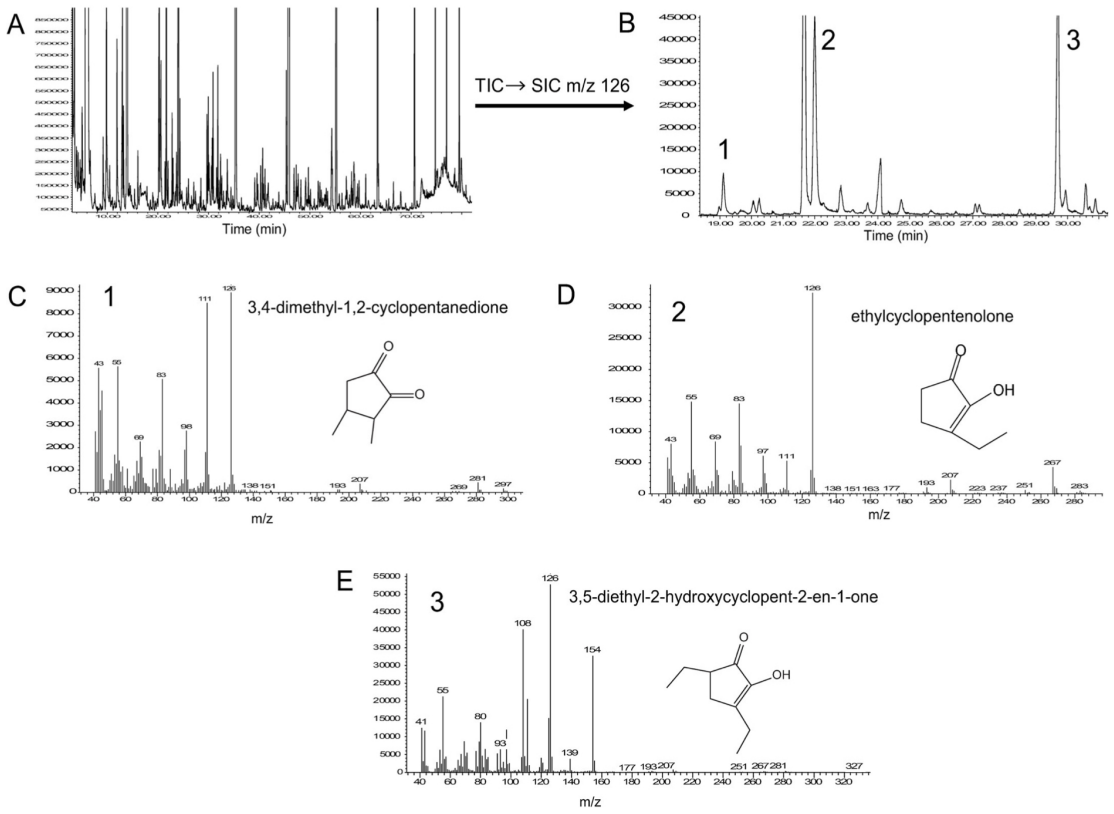

Fig 4. High loading compounds on sweat PC1 and their mass spectra (EI 70 eV). (A) Total ion chromatogram (TIC); (B) Post-run extracted m/z 126 single ion current chromatogram (SIC); (C) Compound 1, 3,4-dimethyl-1,2-cyclopentadione from SIC at retention time 16.1 min; (D) Compound 2, ethylcyclopentenolone from SIC at retention time 22.02 min; (E) 3,5-diethyl- 2-hydroxycyclopent-2-en-1-one from SIC at retention time 29.69 min.

Abstract: Excessive home cage aggression often results in severe injury and subsequent premature euthanasia of male laboratory mice. Aggression can be reduced by transferring used nesting material during cage cleaning, which is thought to contain aggression appeasing odors from the plantar sweat glands. However, neither the composition of plantar sweat nor the deposits on used nesting material have been evaluated. The aims of this study were to (1) identify and quantify volatile compounds deposited in the nest site and (2) determine if nest and sweat compounds correlate with social behavior. Home cage aggression and affiliative behavior were evaluated in 3 strains: SJL, C57BL/6N, and A/J. Individual social rank was assessed via the tube test, because ranking may influence compound levels. Sweat and urine from the dominant and subordinate mouse in each cage, plus cage level nest samples were analyzed for volatile compound content using gas chromatography-mass spectrometry. Behavior data and odors from the nest, sweat, and urine were statistically analyzed with separate principal component analyses (PCA). Significant components, from each sample analysis, and strain were run in mixed models to test if odors were associated with behavior. Aggressive and affiliative behaviors were primarily impacted by strain. However, compound PCs were also impacted by strain, showing that strain accounts for any relationship between odors and behavior. C57BL/6N cages displayed the most allo-grooming behavior and had high scores on sweat PC1. SJL cages displayed the most aggression, with high scores on urine PC2 and low scores on nest PC1. These data show that certain compounds in nesting material, urine, and sweat display strain specific patterns which match strain specific behavior patterns. These results provide preliminary information about the connection between home cage compounds and behavior. Salient compounds will be candidates for future controlled studies to determine their direct effect on mouse social behavior.